ISSN 1392 - 1207. MECHANIKA. 2014 Volume 20(1): 70-79

Application of Ni-Ti shape memory alloy actuators in a walking micro-robot

I. Doroftei*, B. Stirbu**
**Gheorghe Asachi Technical University of Iasi, B-dul D. Mangeron 61-63, 700050 Iasi, Romania,*
E-mail: idorofte@mail.tuiasi.ro
***Gheorghe Asachi Technical University of Iasi, B-dul D. Mangeron 61-63, 700050 Iasi, Romania,*
E-mail: bogdanstirbu@yahoo.com

crossref http://dx.doi.org/10.5755/j01.mech.20.1.3531

1. Introduction

One of the limitations of current wheeled/legged locomotion mechanisms is that they are designed to access only certain terrains. On the other hand, complex drive mechanisms for motion transmission make them more vulnerable to failure possibilities. Also, in order to miniaturize the mobile robots and make them in a scalable manufacturing technique, mechanisms other than wheels are required. Wheels, even with the most innovative suspension mechanisms, can negotiate obstacles with height at most twice the wheel diameter. This is why the development of alternate locomotion mechanisms become quite necessary, especially as the size of the mobile robot is reduced. Advanced flexible actuators will allow the design of direct-driven limbs (legs/muscles/appendages) bypassing the need for complex chassis (motors and drive systems). The limbs will possess the added advantage of reconfigurability, with substantially lesser mechanical vulnerability [1].

The research in walking mechanisms is one of the challenges in mechanical engineering and mechatronics. Although wheeled vehicles are very familiar and everywhere around us, legged robots are preferred because of their superior mobility in unstructured terrain [2-6].

As we know, biological mechanisms like legs with high effectiveness and developing high forces are very common in nature. This is why introducing such structures in robotics is one of the most popular research in biomimetics.

Legged animals in general and insects in particular can be found everywhere in nature. They are well known not only for their speed and agility but also for their ability to traverse some of the most difficult terrains, climbing vertical surfaces, or even walking upside down [7]. This is a reason for which researchers are fascinated to build legged insect-like systems, to cross difficult terrain and to be useful in dangerous environments, for special applications. A hexapod walking robot is an example of such insect-like vehicle and shape memory alloy (SMA) wires are a flexible actuators category suitable for biomimetic systems [8-11].

As robots are requested to perform tasks in rough terrain, the development of actuators capable to flexibly adapt to the unstructured environment becomes more and more necessary. The conventional mechanisms with stiff joints make the robots more complex, heavy, large and expensive. In these conditions, the development of small and low cost actuators which can flexibly adapt to unstructured environment becomes desirable.

Different types of actuators may be used for a robot driving. Electrical, hydraulical and pneumatical actuators are so called conventional because they are commonly used to actual robot systems. Recent research in the field of materials discovered some new light and resistant alloys, which allow building compact, light and resistant articulated mechanisms. Such intelligent materials could be used to develop new actuators [10], [12-14].

A wide variety of artificial muscles have been investigated. Shape Memory Alloys (SMAs) are a category of such artificial muscles which can be used as actuators in the structure of a biomimetic walking robot.

In 1938, Arne Olander, a Swedish physicist, was the first who observed the pseudo elastic behavior of the gold-cadmium alloy [15]. He observed how the alloy could be plastically deformed when cool, but return to its original length when heated. Kurdjumov and Khandros [16] conducted experiments on copper-zinc and copper-aluminium alloys and introduced the concept of thermo elastic martensitic transformation to explain the reversible transformation of martensite.

The real breakthrough in the research and the application of shape memory alloys is the discovery of nickel-titanium (NiTi) by Buehler et al. [17] in 1963. The alloy was termed Nitinol, an acronym of nickel (NI), titanium (TI) and Naval Ordnance Laboratory (NOL). In addition, the term 'shape memory effect' was first introduced to describe the shape recovery behaviour of the alloy.

The first commercially available application involved the use of Nitinol material for pipe coupling in F-14 fighter aircraft [18]. Nitinol has been widely used in biomedical applications due to its biocompatibility [19]. Some common areas of use are in medical stents, implants and orthodontics [20, 21]. However, it wasn't until the 1990's that research into the use of Nitinol SMAs as actuators in robotics and prosthetics began to take hold. Actuator applications include linear actuators, microswitches, robotic grippers and micro-electromechanical devices (MEMS) [22].

There are some properties of SMAs which have motivated their use as in a biomimetic actuation system: SMAs are compact, light-weight, with a high power to mass ratio; these actuators are direct-driven, so they are commonly used in the form of wires that are activated through resistive heating (by using an electric current) with no need for complex and bulky transmission systems; SMA actuators operates with no friction or vibration allowing extremely silent movements. They can exhibit large changes in shape when heated and cooled and can replace

motors and solenoids for creating motion in many devices, even robots. SMA based actuators have been successfully used in many robotic applications till now [7], [11], [23-40].

However, these actuators also have limitations which need to be considered before applying them in any robotic system: A large portion of the power applied is dissipated as heat leading to low power efficiencies; the speed of actuation is dependent upon the rate of cooling of the wire leading to low bandwidths; even though SMAs exhibit relatively large strains (8% for Nitinol), only a fraction of the net strain can be utilized in order to maximize the actuator lifetime.; clever designs that convert the small strains into large motions are required. SMA contraction is highly non-linear owing to temperature hysteresis during joule heating of the material. As such, SMAs actuators are difficult to effectively control.

The present work was carried out in order to design and build a walking micro-robot using Ni-Ti SMA wires as actuators.

2. SMA based actuators

Actuators are the most critical components in animal-like robot conception. Neuro-muscular systems of animals are using totally different control techniques comparing to those used to control conventional actuators in robotics. Animals ensure the leg joints motion by alternating the contraction of an antagonistic muscles pair and regulate their stiffness by simultaneous contraction of these muscles [1], [14], [23], [29], [41-42].

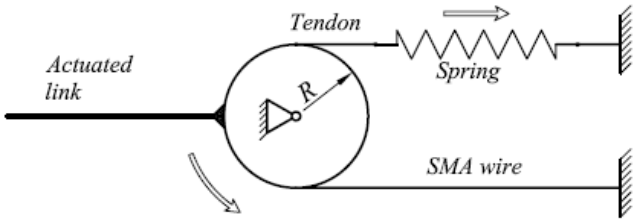

a

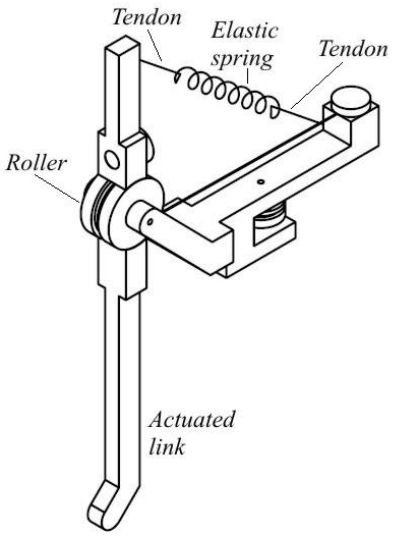

b

Fig. 1 Bias spring-type SMA based actuator: a) kinematics; b) constructive solution

Because in the structure of biological walking mechanisms we find rotational joints, when we design actuators based on SMA, such kind of joints will be taken into account. There are many SMA actuator solutions but only two of them have been used in the designs described in this paper. The first one is the bias spring-type actuator (Fig. 1).

In the case of a hexapod walking micro-robot, this actuator can be used to move the leg up and down. Using it to rotate the leg around the vertical axis, the robot will only move in one direction (the force developed by the bias spring will not be capable to move the robot in opposite direction).

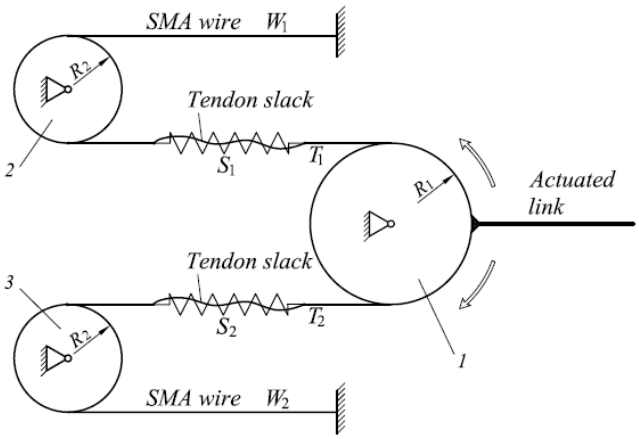

a

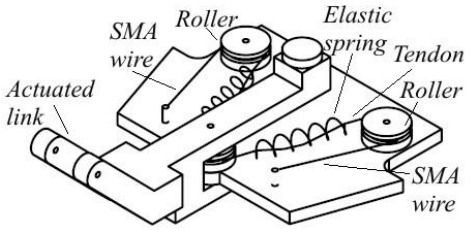

b

Fig. 2 Bidirectional SMA based actuator: a) kinematics; b) constructive solution

In order to improve robot mobility and leg compliance, another solution of actuator is proposed (Fig. 2). This is a bidirectional actuator based on two SMA wires, two elastic springs and two tendons, based on the solution adopted by [23], [29]. The spring S_2 biases the SMA wire W_1, whereas the spring S_1 biases SMA wire W_2. Counter-clockwise link rotation occurs by the contraction of W_1 wire whereas clockwise link rotation occurs by the contraction of W_2 wire. As the wire W_1 contracts, for example, the spring S_1 expands, absorbing the slack in the tendon T_1 until it is fully stretched and taut. Whereas the actuated link can rotate in counter-clockwise direction during the absorbing of the slack, depending of the spring stiffness, at the point where the tendon is stretched and taut, any further contraction of the SMA wire W_1 will act directly on the actuated link, rotating it in the mentioned direction. Simultaneously, as the actuated link is rotating, the spring S_2 expands and the slack in the tendon T_2 is absorbed. When the SMA wire W_1 is deactivated, the springs S_1 and S_2 will return to their original positions and the actuated link will return to its neutral position. When the wire W_2 is acti-

vated, the link is rotating in clockwise direction.

This solution, with spring-slack artificial tendons, mimics the nonlinear stiffness of the natural tendons. Whereas the nonlinear stiffness of the biological tendons limits the motion range of the natural links, the limit on the range of motion of the artificial joint is dependent on two factors:

- the SMA wire's stroke range must be sufficiently large to first absorb the slack in the active tendon to which it is connected in order to produce joint rotation;
- the link cannot rotate beyond the elastic limit of the opposing tendon.

Two defining criteria come into play when selecting the SMA actuator:

- the actuator stroke and
- the output force.

The SMA wire contraction length must be sufficient to pull the link throughout its full range of motion about the joint axis. Also, the force output of the SMA actuator must produce joint torques, which are high enough to maintain the robot in static equilibrium.

The SMA actuator force, necessary to generate the joint torque, can be derived from the static equation of motion for a given link. Consider the forces acting on the link, taking into account the bias spring SMA actuator, as shown in Fig. 3. This actuator can be used to move the leg up and down.

In a static equilibrium, we have:

$$F_z l \cos\theta = \left(F_{SMA} - F_S\right) R\,, \tag{1}$$

where F_z is vertical contact force of the foot on the ground; F_{SMA} is the force in the SMA wire; $F_S = k \times \Delta x$ is elastic force in the spring; l is the link length; R is roller radius; θ is angular stroke of the joint.

Starting from Eq. (1), the force in the SMA wire will be:

$$F_{SMA} = \frac{F_z l}{R}\cos\theta + k\left(R\theta + \Delta x\right), \tag{2}$$

where k is the spring constant; Δx is spring elongation.

For the bidirectional SMA based actuator, we will consider Fig. 4, for counter-clockwise rotation, when the SMA wire W_1 is active. This actuator is used to rotate the leg around the vertical axis, moving it forward and backward.

The static equilibrium for counter-clockwise rotation leads to:

$$F_1 R_1 = F_2 R_1 + F_x l \cos\alpha\,, \tag{3}$$

where F_x is horizontal contact force of the foot; μ is friction coefficient; $F_1 = F_{SMA_1} - F_{S_1}$ is force in tendon T_1; $F_2 = F_{S_2}$ is force in tendon T_2; R_1 is radius of the roller 1; α is angular stroke of the joint for counter-clockwise rotation.

But

$$F_{S_1} = k\left(\Delta l_1 + \Delta x\right) = k\left(R_1\frac{\theta}{2} + \Delta x\right), \tag{4}$$

$$F_{S_2} = k\left(\Delta l_2 + \Delta x\right) = k\left(R_1\frac{\theta}{2} + \Delta x\right), \tag{5}$$

where k is the elastic constant of the springs; Δx is their elongation.

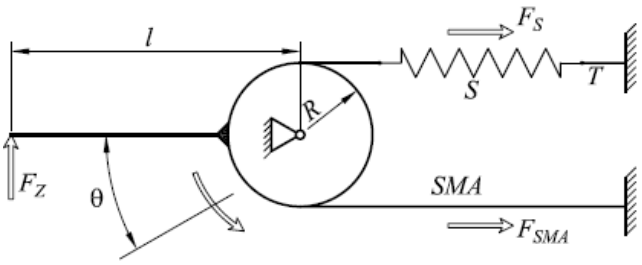

Fig. 3 Forces acting on the link - bias spring SMA actuator

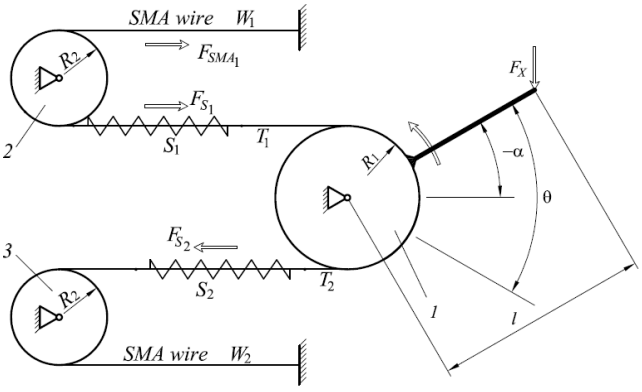

Fig. 4 Forces acting on the link - bidirectional SMA actuator, counterclockwise rotation

The horizontal contact force F_x will be considered for the most unfavourable situation, that of the tripod gait. It is:

$$F_x = \mu F_z\,, \tag{6}$$

where μ is the friction coefficient between the foot and the ground.

If we replace F_1 and F_2 in Eq. (3), we get:

$$F_{SMA_1} = k\left(R_1\theta + 2\Delta x\right) + \frac{\mu F_z l}{R_1}\cos\alpha\,, \tag{7}$$

with $\alpha \in \left[0,\ \theta/2\right]$.

Eq. (7) is valid for the second situation too, when we consider the link rotation in clockwise direction.

The motion generated by an actuator based on SMA wires is the result of the axial strain in the wire, due to the martensite/austenite transformation phase. Maximal axial strain σ_{max} in a Ni-Ti wire is approximately 400 MPa. In these conditions, the maximum torques developed in a rotational joint, actuated by a number of n SMA wires with d diameter, is:

$$\tau_{max} = nR_r\sigma_{max}\frac{\pi d^2}{4}\,, \tag{8}$$

where R_r is the roller radius.

If the maximum torque σ_{max} is imposed, the num-

ber of wires with d diameter may be computed:

$$n = \frac{4\tau_{max}}{\pi R_r d^2 \sigma_{max}}, \tag{9}$$

or the wires diameter d if the number of wires is known,

$$d = \sqrt{\frac{4\tau_{max}}{\pi n R_r \sigma_{max}}}. \tag{10}$$

At first glance, it would seem that the best would be to use a smaller number of larger diameter wires. However, the diameter of wire affects the reaction rate. This is why, to reduce the response time, a bigger number of smaller diameter wires is preferable to be used.

3. Leg mechanisms

The number of degrees of freedom (DOF) provided for each leg seems to be a compromise between an increased range of motion of the leg and a control simplicity. However, that turns out not to be the case. Only leg designs having two DOF or three DOF were considered, since more than three DOF provides no additional benefits comparing to the additional complications in control that would arise [6], [35].

Legs with two DOF provide a relatively simple control system, because there is one less actuator, if we compare them with legs with three DOF However, with only two DOF, it is very difficult to achieve the above-stated fixed goal of arbitrary navigation on a plane surface.

These legs require a walking gait where the feet slip along the ground, if they are to travel in curved paths as well as travel straight ahead [2-5], [10], [34], [42]. This is undesirable from a control standpoint, though, because systematic slippage of the feet implies that the robot's position no longer can be tracked by feedback from the motor controllers. Additional sensors would be necessary to track the motion of the robot's body over the ground. Although the trajectory of a robot using legs with two DOF can never be a straight line because of the kinematics, the slippage does not cause any particular mechanical problem when the robot has a small weight [2-5], [10].

On the other hand, with three DOF per leg, the foot can be positioned anywhere within a three-dimensional workspace [34], [42]. This means that using six such legs the robot can navigate in either a straight or curved path over uneven terrain to reach any point on the terrain surface.

A first solution of two DOF (θ_1 and θ_2) serial leg based on one bias spring-type SMA actuator and one bidirectional SMA actuator is shown in Figure 5. Because we want to amplify the small strains of the SMA wires, some pulleys are inserted in each link design of the leg.

If we apply the standard Denavit-Hartenberg convention in Fig. 5, a we may find the coordinates of O_2 according to the referential origin, O_0,

$$\begin{cases} x_{2-0} = \left(-l_1 - l_2 \sin\theta_2\right)\sin\theta_1; \\ y_{2-0} = \left(l_1 + l_2 \sin\theta_2\right)\cos\theta_1; \\ z_{2-0} = -l_2 \cos\theta_2. \end{cases} \tag{11}$$

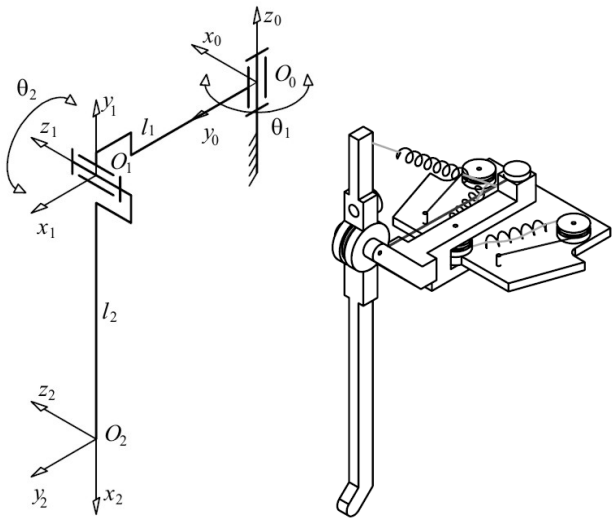

a b

Fig. 5 Serial leg with two DOF: a) kinematics; b) constructive solution

We need these coordinates in order to compare the performances of the proposed leg mechanisms. When SMA actuators are using, clever designs that convert the small strains into large motions are required. Taking into account this fact, a new two DOF leg based on a mechanism with a tree structure (with one closed loop) is proposed (Fig. 6). This leg is using a bias spring-type SMA actuator for θ_2 joint and one bidirectional SMA actuator for θ_1 joint. It means that this leg will have compliance for rotation around z_0 axes.

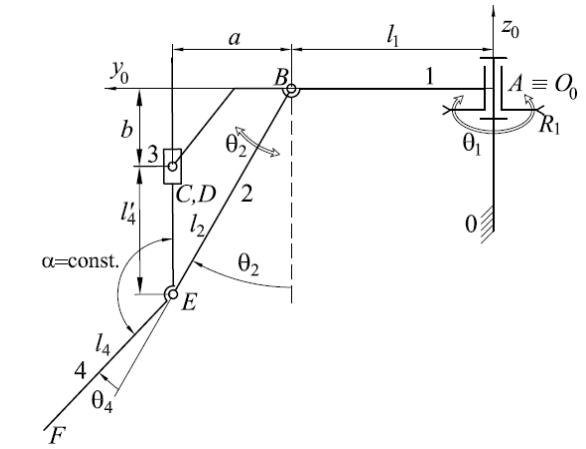

a

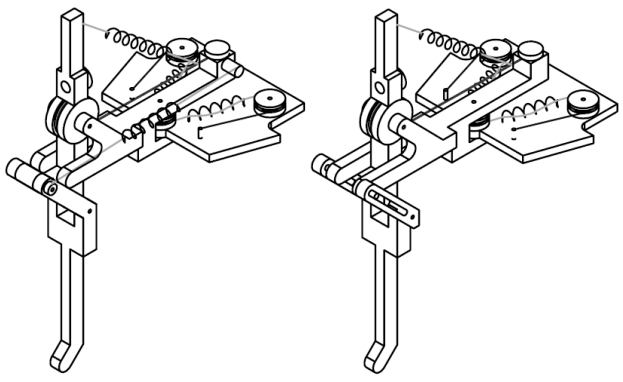

b c

Fig. 6 Leg with two active DOF and tree structure: a) kinematics; b) one constructive solution; c) the second constructive solution

Direct kinematics for this leg leads to next equations:

$$\begin{cases} x_F = \left(-l_1 - l_2\, sin\,\theta_2 - l_4\, sin\left(\theta_2+\theta_4\right)\right) sin\,\theta_1; \\ y_F = \left(l_1 + l_2\, sin\,\theta_2 + l_4\, sin\left(\theta_2+\theta_4\right)\right) cos\,\theta_1; \\ z_F = -\,l_2\, cos\,\theta_2 - l_4\, cos\left(\theta_2+\theta_4\right), \end{cases} \quad (12)$$

with

$$\theta_4 = atan\left(\frac{a - l_2\, sin\,\theta_2}{b - l_2\, cos\,\theta_2}\right) + \pi - \alpha - \theta_2 . \quad (13)$$

In order to prove the advantage of the leg with tree structure (Fig. 6) comparing to the serial one (Fig. 5), a numerical simulation in Matlab has been done, computing the vertical stroke Δz of the tip legs. The next values of the constructive and kinematic parameters have been considered for the serial leg: $l_1 = 20$ mm, $l_2 = 55$ mm, $\theta_1 = -15$ to 15 degrees, $\theta_2 = 0$ to 30 degrees. For the second leg (Fig. 6), the next parameters have been considered: $l_1 = 20$ mm, $l_2 = 16.75$ mm, $l_4 = 38.25$ mm, $a = 5$ mm, $b = 10$ mm, $\theta_1 = -15$ to 15 degrees, $\theta_2 = 0$ to 30 degrees. In order to get a real comparison of the two legs, the sum l_2+l_4 for the second leg is equal to l_2 of the first leg.

The results of the simulation are shown in Fig. 7. If we compare the two diagrams, we can see that the leg with tree structure has a vertical stroke of its tip four times bigger than that of a serial leg structure. It means that, for the same vertical stroke of the leg tip, the length of the wire used for θ_2 joint should be much smaller for a leg with tree structure.

This will lead to less power consumption and smaller volume of the SMA actuator. Or, if we consider using the same length of the SMA wire for both leg solutions, the robot using legs with tree structure could climb obstacles four times higher.

If the global dimensions of the leg are known (lengths l_1, l_2, l_4 are imposed), the vertical stroke of the leg tip is influenced by two constructive parameters (a and b). The influence of these parameters on the coordinate z_F is shown in Fig. 8.

If we derivate the Eq. (12) by time, we get:

$$\begin{bmatrix} \dot{x}_F \\ \dot{y}_F \\ \dot{z}_F \end{bmatrix} = J \times \begin{bmatrix} \dot{\theta}_1 \\ \dot{\theta}_2 \\ \dot{\theta}_4 \end{bmatrix}, \quad (16)$$

where J is the analytical Jacobian matrix:

$$J = \begin{bmatrix} \begin{pmatrix} -l_1 - l_2 s_2 - \\ -l_4 s_{24} \end{pmatrix} c_1 & \begin{pmatrix} -l_2 c_2 - \\ -l_4 c_{24} \end{pmatrix} s_1 & -l_4 s_1 c_{24} \\ \begin{pmatrix} -l_1 - l_2 s_2 - \\ -l_4 s_{24} \end{pmatrix} s_1 & \begin{pmatrix} l_2 c_2 + \\ +l_4 c_{24} \end{pmatrix} c_1 & l_4 c_1 c_{24} \\ 0 & l_2 s_2 + l_4 s_{24} & l_4 s_{24} \end{bmatrix} \quad (17)$$

and $s_1 = sin\,\theta_1$, $c_1 = cos\,\theta_1$, $s_2 = sin\,\theta_2$, $c_2 = cos\,\theta_2$, $s_{24} = sin\left(\theta_2+\theta_4\right)$, $c_{24} = cos\left(\theta_2+\theta_4\right)$.

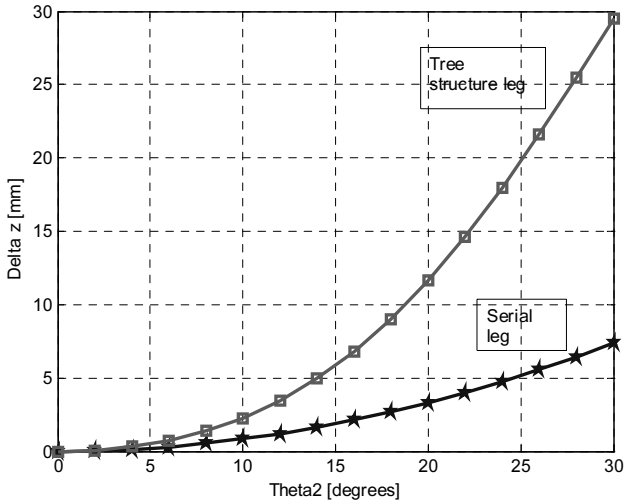

Fig. 7 Diagram $\Delta z = f\left(\theta_2\right)$

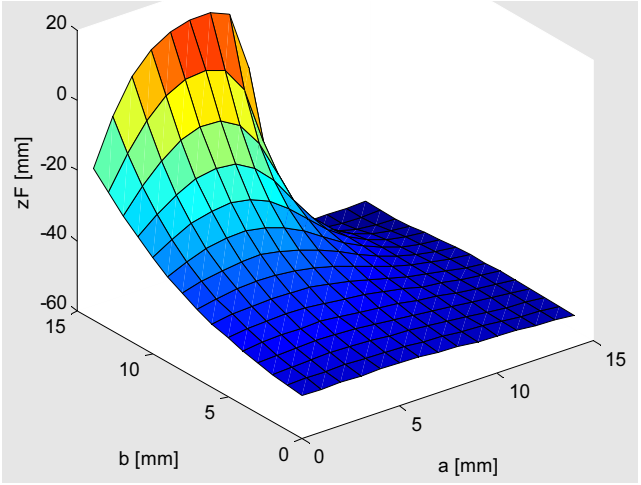

Fig. 8 The influence of a and b parameters on the z_F coordinate

In order to get the torque for each joint, next equation could be used:

$$\tau = J^T F , \quad (18)$$

with $\tau = \left[\tau_1, \tau_2, \tau_4\right]^T$, $F = \left[F_x, F_y, F_z\right]^T$ (F_x, F_y, F_z are the contact forces at the leg tip).

If we know the contact forces at the extremity of the leg, we may compute

$$\begin{bmatrix} \tau_1 \\ \tau_2 \\ \tau_4 \end{bmatrix} = \begin{bmatrix} \begin{pmatrix} -l_1 - l_2 s_2 - \\ -l_4 s_{24} \end{pmatrix} c_1 & \begin{pmatrix} -l_1 - l_2 s_2 - \\ -l_4 s_{24} \end{pmatrix} s_1 & 0 \\ \begin{pmatrix} -l_2 c_2 - \\ -l_4 c_{24} \end{pmatrix} s_1 & \begin{pmatrix} l_2 c_2 + \\ +l_4 c_{24} \end{pmatrix} c_1 & l_2 s_2 + l_4 s_{24} \\ -l_4 s_1 c_{24} & l_4 c_1 c_{24} & l_4 s_{24} \end{bmatrix} \times \begin{bmatrix} F_x \\ F_y \\ F_z \end{bmatrix}. \quad (19)$$

This means, we have the torques in the active joints, τ_1 and τ_2. We use this torques to compute the SMA wire diameter and the number of wires for each actuator. The joint θ_4 is passive and it does not require an actuator.

4. Micro-robot design and implementation

Based on the second leg mechanism discussed above, a solution of biomimetic walking micro-robot is proposed, using SMA as actuators and springs, in order to imitate the compliance of biological mechanisms. The design solution (Fig. 9) is based on a leg mechanism with two DOF, actuated by one bias-spring SMA actuator and one differential actuator. Thanks to the second actuator, the leg has an artificial compliance for horizontal movement.

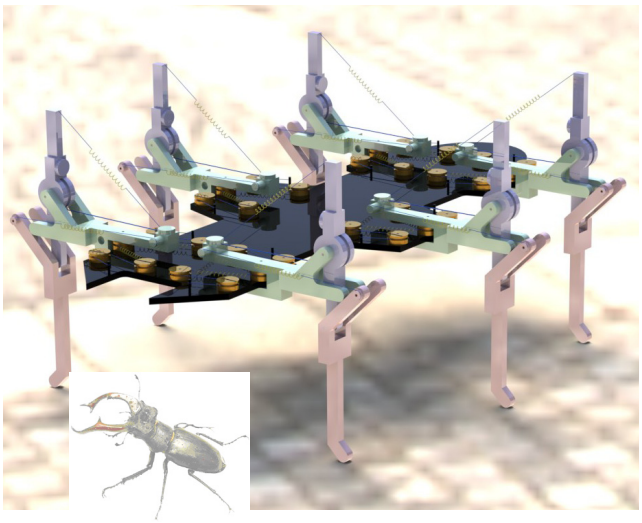

Fig. 9 A 3D view of the hexapod walking micro-robot

Six legs offer a good compromise between weight and electromechanical complexity, on one hand, and stability, velocity and the variety of gaits, on the other hand. Each of the six legs was equipped with only two active degrees of freedom, in order to minimize its complexity. Although the trajectory can never be a straight line because of the kinematics, the slippage does not cause any particular mechanical problem because of the small weight of the vehicle.

Direct kinematics of the robot expresses the coordinates of the tip feet with respect to the referential centre (geometrical centre of the robot body):

$$\begin{cases} x_i = l_0 + \left(l_1 + l_2 \sin\theta_{2\_i} + l_4 \sin\left(\theta_{2\_i} + \theta_{4\_i}\right)\right)\sin\theta_{1\_i}; \\ y_i = l'_0 + \left(l_1 + l_2 \sin\theta_{2\_i} + l_4 \sin\left(\theta_{2\_i} + \theta_{4\_i}\right)\right)\cos\theta_{1\_i}; \\ z_i = l''_0 - l_2 \cos\theta_{2\_i} - l_4 \cos\left(\theta_{2\_i} + \theta_{4\_i}\right), \end{cases} \quad (22)$$

where $i = 1\ldots6$ denotes the leg indices; l_0 and l'_0 are the distances between robot centre of mass and the axis of joints θ_{1_i}, on longitudinal and transversal direction; l'_0 is positive for left legs and negative for right legs; θ_{1_i} and θ_{2_i} are the angular strokes of the active joints; θ_{4_i} is computed using Eq. (13).

These coordinates are useful if we want to compute the contact forces between the feet tip and the ground. We need these forces to compute the actuators torques and, then, to select the optimum SMA actuator (the diameter of the wire and the number of SMA wires).

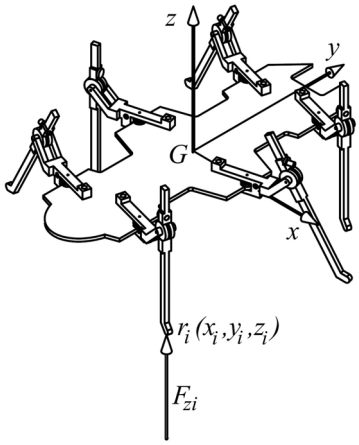

Fig. 10 Force distribution for a given gait state

As a first step of the contact forces calculus, the force distribution for a given gait state of the robot can be computed, by expressing the static equilibrium equations of the whole vehicle. In order to simplify these equations, we assume that [4]:

- the speed of the robot and its mass are small enough as well as dynamical effects could be neglected;
- the ground support forces are vertical (Fig. 10);
- the mass of the leg link is negligible comparing to the mass of its actuators and also comparing to the mass of robot body. In other studies, the mass of all the leg is neglected. In our case, the mass of all the six legs is comparable with the mass of the robot body; this is why we consider that the influence of the leg mass should be taken into account.

Assuming that the mass of the robot body, M_b, its centre of mass $(x_b,\ y_b)$, the mass of a leg, m_l and the coordinates of their centres of mass $(x_{l_i},\ y_{l_i})$ are known, and assuming that all the six legs have the same mass, we get:

$$\begin{cases} G = \left(M_b + 6m_l\right)g; \\ G\,x_G = m_l g \sum_{i=1}^{6} x_{l_i}; \\ G\,y_G = m_l g \sum_{i=1}^{6} y_{l_i}, \end{cases} \quad (23)$$

where G is the weight of the vehicle, in N; $i = 1\ldots6$, expresses the leg indices; $(x_G,\ y_G)$ are the coordinates of the robot centre of mass.

If we know θ_{1_i} and θ_{2_i}, we can compute x_{l_i}, y_{l_i}, for $i = 1\ldots6$, at any moment and then $(x_G,\ y_G)$.

Assuming that the ground support forces are vertical, we get:

$$\begin{cases} \sum_{i\in I} F_{z_i} = \left(M_b + 6m_l\right) g; \\ \sum_{i\in I} F_{z_i \cdot x_i} = m_l g \sum_{i=1}^{6} x_{l_i}; \\ \sum_{i\in I} F_{z_i} y_i = m_l g \sum_{i=1}^{6} y_{l_i}, \end{cases} \tag{24}$$

$$[G] = \begin{bmatrix} G \\ m_l g \sum_{i=1}^{6} x_{l_i} \\ m_l g \sum_{i=1}^{6} y_{l_i} \end{bmatrix}. \tag{28}$$

where I is the set of supporting legs (we may have three to six legs on the ground, according to the gait and its phase); x_i, y_i, for $i = 1\ldots6$, are the coordinates of the tip feet with respect to the referential centre (geometrical centre of the robot body).

The Eq. (24) can be rewritten as follow:

$$[A] \times [F_z] = [G], \tag{25}$$

with

$$[A] = \begin{bmatrix} 1 & 1 & 1 & 1 & 1 & 1 \\ x_1 & x_2 & x_3 & x_4 & x_5 & x_6 \\ y_1 & y_2 & y_3 & y_4 & y_5 & y_6 \end{bmatrix}; \tag{26}$$

$$[F_z] = \begin{bmatrix} F_{z_1} & F_{z_2} & F_{z_3} & F_{z_4} & F_{z_5} & F_{z_6} \end{bmatrix}^T; \tag{27}$$

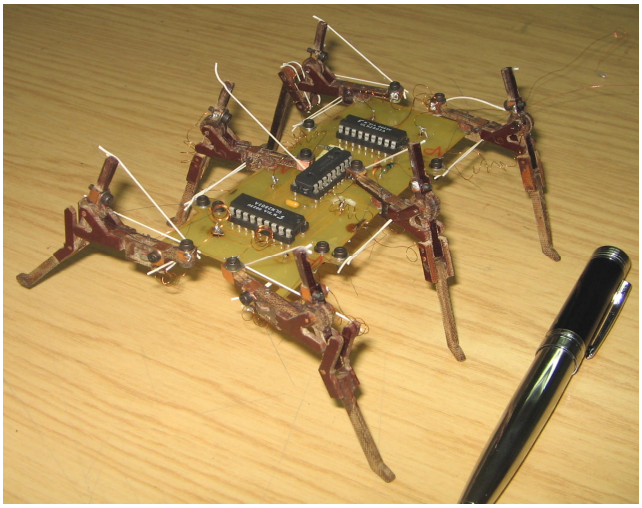

Fig. 11 Picture of the real hexapod micro-robot

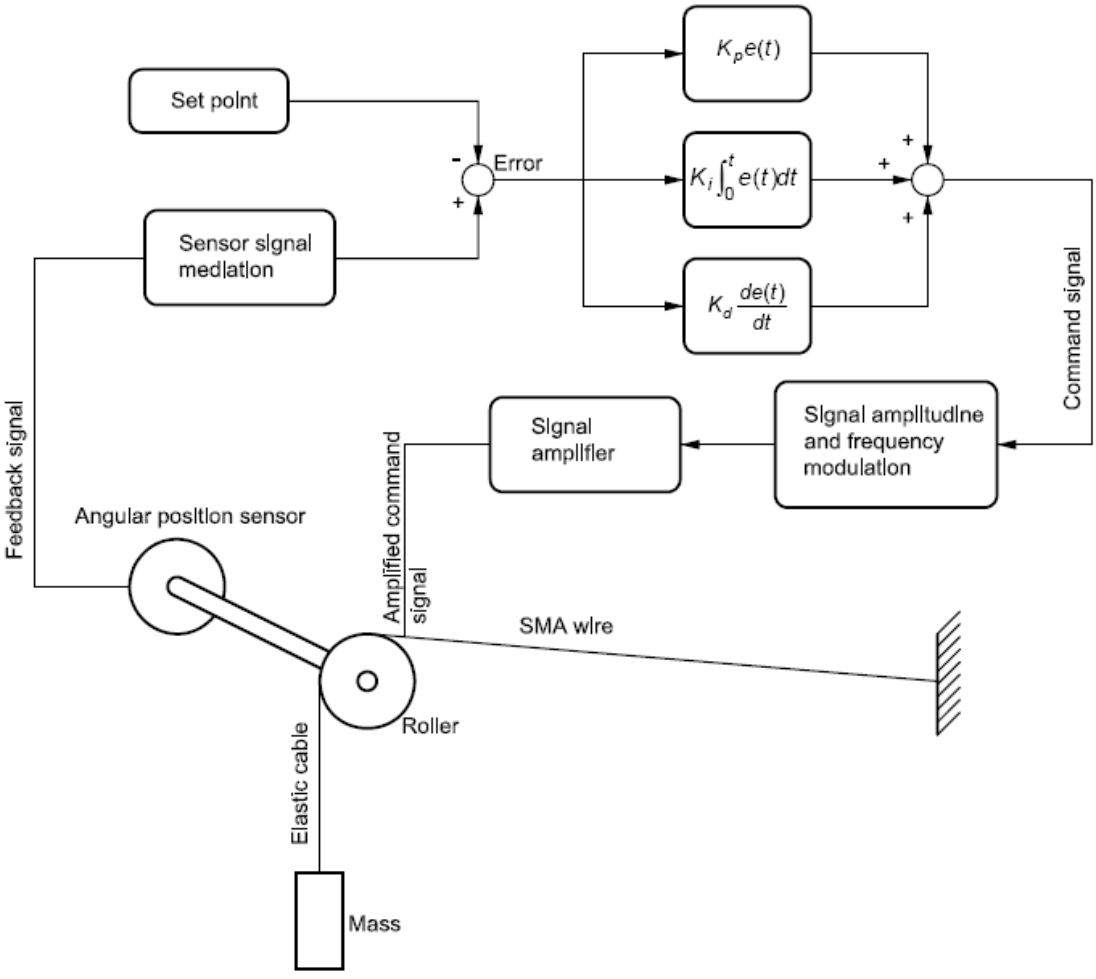

Fig. 12 Single joint closed-loop control scheme

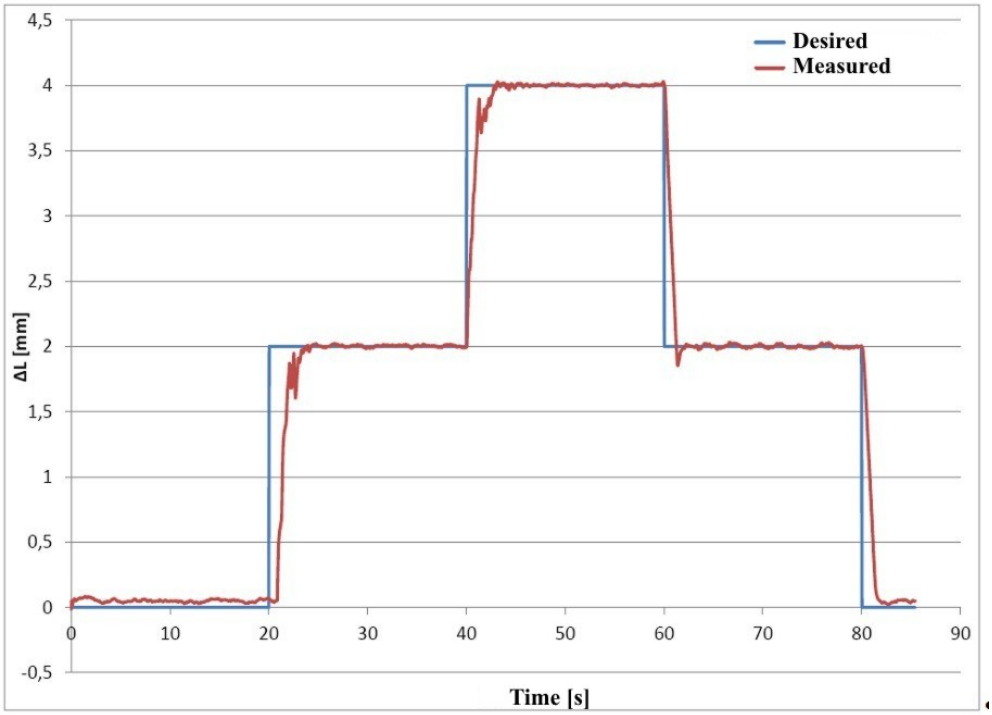

Fig. 13 Closed-loop control of SMA wire deformation

A picture of the real micro-robot is shown in Fig. 11. Both leg solutions have been used for the real micro-robot, in order to highlight the advantages of the legs with tree structure.

The movement of the robot is achieved by heating small shape memory alloy wires (muscle wires) of 50 µm diameter, which are attached to each leg of the micro-robot. Elastic rubber wires are used to return the links of the leg to the initial position, when the muscle wires are no more powered.

Although the trajectory can never be a straight line because of the simple kinematics, the slippage does not cause any particular mechanical problem because of the small weight of the vehicle. Thanks to the small diameter of the SMA wires, a cycle time of about 1 sec can be achieved.

All the legs are mounted directly on the electronic board without any other frames, in order to simplify the architecture of the robot.

The rotating angles of the links depend of the leg structure but also of the value of the wires deformations. So, for a given leg structure, the value of the rotating angle depends directly of the length of the muscle wire. In order to increase the lengths of the wires (to increase the strokes of the legs) and to keep small overall dimensions for the robot, some pulley wheels are integrated in the structure of the leg.

Thanks to a control board based on a 8-bit microcontroller, the robot can walk forward/backward and turn left/right. Since the bit number of the microcontroller is limited to 8, only the tripod gait was implemented here. Because not any encoder is used in the leg joints of this prototype, open-loop control tests were first performed to assess the effectiveness of the actuation mechanisms designed.

In order to adapt the robot to an unstructured environment, position of each rotational joint of the legs has to be controlled, which means a closed loop control of SMA wires deformation.

Taking into account the small dimensions of the links, the use of encoders in robot joints was not possible at this time. This is why a test bench with a bigger constructive solution of a rotational joint has been used to test a closed-loop procedure. The control method is based on heating the SMA wire using a PID controller with squared voltage signal having variable frequency and amplitude (Fig. 12). Different tests performed demonstrated the effectiveness of this method. Because of the lack of space, in this paper only the results of one test will be presented. Fig. 13 shows the results of the wire control deformation for three different angular positions of the actuated joint.

5. Conclusions

Biological mechanisms like legs with high effectiveness and developing high forces are very common in nature. This is why introducing such structures in robotics is one of the most popular research in biomimetics. Shape Memory Alloys are a category of artificial muscles which can be used as actuators in the structure of a biomimetic walking robot. When SMA wires are used, smart mechanisms to amplify their deformation are necessary. In this paper, mechanisms that can convert the small strain of a SMA wire into large motion, used as legs for a hexapod walking micro-robot, have been discussed. Two leg mechanisms have been compared, a serial one and another based on a tree structure. Both numerical and virtual simulations have been proved the advantages of the second solution. Based on these leg mechanisms, a solution of biomimetic walking micro-robot has been proposed, using SMA as actuators and springs, in order to imitate the compliance of biological mechanisms. Then, a test bench for a SMA actuated rotational joint has been used to test a closed-loop procedure. The control method is based on heating the SMA wire using a PID controller with squared voltage signal having variable frequency and amplitude.

Different tests performed demonstrated the effectiveness of this method. Because of the lack of space, in this paper only the results of one test have been presented.

References

1. **Thakoor, S.** 1997. Microexplorers - Final Report, JPL D - 14879A.
2. **Alexandre, P.; Doroftei, I.; Preumont, A.** 1998. An autonomous micro walking machine with articulated body, Proceedings of the 3rd IFAC Symposium, IAV'88: 557-562.
3. **Doroftei, I.; Preumont, A.** 1999. Development of an autonomous micro walking robot with articulated body, Proceedings of the 2nd International Conference on Climbing and Walking Robots, CLAWAR '99: 497-507.
4. **Doroftei, I.; Stirbu, B.; Plesu, Gh.** 2011. Force distribution for a walking robot with articulated body, In: Lovasz EC, Corves B, editors. Mechanisms, Transmissions and Applications, Mechanisms and Machine Science 3(2): 77-89. http://dx.doi.org/10.1007/978-94-007-2727-4_7.
5. **Preumont, A.; Alexandre, P.; Doroftei, I.; Goffin F.** 1997. A Conceptual walking vehicle for planetary exploration, Mechatronics 7(3): 287-296. http://dx.doi.org/ 10.1016/S0957-4158(96)00043-8.
6. **Savant, A.** 2003. Leg design of walking robots, Fr. C. Rodrigues Institute of Technology, Mumbai University, Mechanical Engineering Department, Bs Report, 180p.
7. **Kinglesley, D.A.** 2005. A Cockroach Inspired Robot with Artificial Muscles, Case Western Reserve University, Dep. of Mechanical and Aerospace Engineering, PhD Thesis, 214p.
8. **Cimpoesu, N.; Stanciu, S.; Doroftei, I.; Ionita, I.; Radu, V.; Paraschiv, P.** 2010. Electrical behavior of a smart Nitinol spring under full time constrain, Optoelectronics and Advanced Materials-Rapid Communications 4(12): 2028-2031.
9. **Delcomyn, F.; Nelson, M.E.** 2000. Architectures for a biomimetic hexapod robot, Robotics and Autonomous System 30: 5-15. http://dx.doi.org/10.1016/S0921-8890(99)00062-7.
10. **Doroftei, I.; Adascalitei, F.** 2012. A hexapod microwalking robot with compliant legs, Applied Mechanics and Materials 162: 234-241. http://dx.doi.org/10.4028/www.scientific.net/AMM.162.234.
11. **Fleischer, J.G.** 1999. A method for biomimetic design of a cooperative mobile robot system to accomplish a foraging task, Master Thesis, Colorado State University, 100 p.
12. **Doroftei, I.; Cloquet, J.M.; Preumont, A.** 2000. A motorless micro walking robot, Proceedings of the 3rd International Conference on Climbing and Walking Robots, CLAWAR '2000: 119-124.
13. **Sun, L.; Huang, W.M.; Ding, Z.; Zhao, Y.; Wang, C.C.; Purnawali, H. et al.** 2012. Stimulus-responsive shape memory materials: A review, Materials and Design 33: 577-640. http://dx.doi.org/10.1016/j.matdes.2011.04.065.
14. **Torres-Jara, E.; Gilpin, K.; Karges, J.; Wood, R.J.; Rus, D.** 2010. Compliant modular shape memory alloy actuators composable flexible small actuators built from thin shape sheets, IEEE Robotics & Automation Magazine 17(4): 78-87. http://dx.doi.org/10.1109/MRA.2010.938845.
15. **Otsuka, K.; Wayman, CM**. 1998. Shape Memory Materials, Cambridge University Press, 282p.
16. **Kurdjumov, G.V.; Khandros, L.G.** 1949. First Reports of the Thermoelastic Behaviour of the Martensitic Phase of Au-Cd Alloys, Doklady Akademii Nauk, SSSR 66: 211-213.
17. **Buehler, W.J.; Gilfrich, J.V.; Wiley, R.C.** 1963. Effects of low-temperature phase changes on the mechanical properties of alloys near composition TiNi, Journal of Applied Physics 34: 1475-1477. http://dx.doi.org/10.1063/1.1729603.
18. **Schetky, L.M.** 1979. Shape memory alloys, Scientific American 241: 74-82. http://dx.doi.org/10.1038/scientificamerican1179-74.
19. **Heisterkamp, C.A.; Buehler, W.J.; Wang, F.E.** 1969. 55-Nitinol: A new biomaterial, Proceedings of the 8th International Conference on Medical & Biological Engineering: 61-64.
20. **Gil, F.J.; Planell, J.A.** 1998. Shape memory alloys for medical applications, Proceedings of the Institution of Mechanical Engineers, Part H: Journal of Engineering in Medicine 212: 473-488. http://dx.doi.org/10.1243/0954411981534231.
21. **Bogue, R.** 2009. Shape-memory materials: A review of technology and applications, Assembly Automation 29(3): 214-219. http://dx.doi.org/10.1108/01445150910972895.
22. **Teh, Y.H.** 2008. Fast, accurate force and position control of shape memory alloy actuators, Ph.D. Thesis, The Australian National University, 179p.
23. **Bundhoo, V.; Haslam, E.; Birch, B.; Park, E.J.** 2009. A shape memory alloy-based tendon-driven actuation system for biomimetic artificial fingers, part I: design and evaluation, Robotica 27: 131-146. http://dx.doi.org/10.1017/S026357470800458X.
24. **Chen, Z.; Shatara, S.; Tan, X.** 2010. Modeling of biomimetic robotic fish propelled by an ionic polymer-metal composite caudal fin, IEEE/ASME Transactions on Mechatronics 15(3): 448-459. http://dx.doi.org/10.1109/TMECH.2009.2027812.
25. **Conrad, J.M.; Mills, J.W.** 1997. Stiquito - Advanced Experiments with a Simple and Inexpensive Robot, Wiley-Blackwell, 328p.
26. **Conrad, J.M.; Mills, J.W.** 1999. Stiquito for Beginners -An Introduction to Robotics, Wiley, John & Sons, Incorporated, 192p.
27. **Elahinia, M.; Ashrafoun, H.** 2002. Nonlinear control of a shape memory alloy actuated manipulator, Transanctions of the ASME. Journal of Vibration and Acoustics 124(4): 566-575. http://dx.doi.org/10.1115/1.1501285.
28. **Esfahani, E.T.; Elahinia, M.H.** 2007. Stable Walking Pattern for an SMA-Actuated Biped, IEEE/ASME Transactions on Mechatronics 12(5): 534-541. http://dx.doi.org/10.1109/TMECH.2007.905707.
29. **Gilardi, G.; Haslam, E.; Bundhoo, V.; Park, E.J.** 2010. A shape memory alloy based tendon-driven actuation system for biomimetic artificial fingers, part II: modelling and control, Robotica 28: 675-687. http://dx.doi.org/10.1017/S0263574709990324.
30. **Gilbertson, R.G.** 1996. Muscle Wires – Project Book,

3rd edition, Mondo-Tronics, Inc. San Anselmo, 128p.
31. **Hoover, A.M.; Steltz, E.; Fearing, R.S.** 2008. RoACH: An autonomous 2.4g crawling hexapod robot, IEEE/RSJ International Conference on Intelligent Robots and Systems, IROS 2008, 26-33. http://dx.doi.org/10.1109/IROS.2008.4651149.
32. **Huang, H.L.; Park, S.H.; Park, J.O.; Yun, C.H.** 2007. Development of stem structure for flower robot using SMA actuators, IEEE International Conference on Robotics and Biomimetics, ROBIO 2007, 15-18.
33. **Liu, S.H.; Huang, T.S.; Yen, J.Y.** 2008. Sensor fusion in a SMA-based hexapod bio-mimetic robot, IEEE International Conference on Advanced Robotics and its Social Impacts, ARSO 2008: 1-6.
34. **MacDonald, W.S.** 1994. Senior Honors Thesis, University of Massachusetts-Amherst, 160p.
35. **Nishida, M.; Tanaka, K.; Wang, H.O.** 2006. Development and control of a micro biped walking robot using shape memory alloys, Proceedings of the IEEE International Conference on Robotics and Automation, 1604-1609.
36. **Price, A.D.; Jnifene, A.; Naguib, H.E.** 2007. Design and Control of a SMA Based Dexterous Robot Hand, Smart Materials and Structures 16: 1401-1414. http://dx.doi.org/10.1088/0964-1726/16/4/055.
37. **Son, H.M.; Gul, J.B.; Park, S.H.; Lee, Y.J.; Nam, T.H.** 2006. Design of new quadruped robot with SMA actuators for dynamic walking, SICE-ICASE International Joint Conference 1-13: 4082-4086.
38. **Sreekumar, M.; Nagarajan, T.; Singaperumal, M.** 2009. Application of trained NiTi SMA actuators in a spatial compliant mechanism: Experimental investigations, Materials and Design 30: 3020-3029. http://dx.doi.org/10.1016/j.matdes.2008.12.017.
39. **Tu, K.Y.; Lee, T.T.; Wang, C.H.; Chang, C.A.** 1999. Design of a fuzzy walking pattern (FWP) for a shape memory alloy (SMA) biped robot, Robotica 17: 373-382. http://dx.doi.org/10.1017/S0263574799001617.
40. **Young, P.L.; Byungkyu, K.; Moon, G.L.; Jong-Oh, P.** 2004. Locomotive mechanism design and fabrication of biomimetic micro robot using shape memory alloy, Proc. IEEE Int. Conf. on Robotics & Automation, 5007-5012.
41. **Ayers, J.; Witting, J.** 2007. Biomimetic approaches to the control of underwater walking machines, Philosophical Transactions: Mathematical, Physical and Engineering Sciences (Series A) 365(1850): 273-295. http://dx.doi.org/10.1098/rsta.2006.1910.
42. **Angle, C.M.** 1991. Design of an Artificial Creature, Master's Thesis, MIT, 121p.

I. Doroftei, B. Stirbu

NI-TI FORMOS ATMINTIES LYDINIO VYKDIKLIO TAIKYMAS ŽINGSNIUOJANČIAJAME MIKROROBOTE

R e z i u m ė

Kadangi žingsniuojantieji robotai tinka darbui nelygiose vietose, didėja poreikis kurti vykdiklius, gebančius lanksčiai adaptuotis nežinomoje aplinkoje. Tradiciniai mechanizmai su standžiomis jungtimis daro robotą kompleksiškesnį, sunkesnį, didesnį ir brangesnį. Formos atminties lydiniai priskiriami dirbtinių raumenų, kurie gali būti naudojami kaip žingsniuojančiųjų robotų aktuatoriai, kategorijai. Net jei šildant ir šaldant jų forma labai keičiasi, aktuatoriaus eksploatavimo trukmei pailginti gali būti panaudota tik viena jų deformuojama dalis. Todėl reikalingi išmanūs mechanizmai, kurie mažas vielos deformacijas keistų į nemažus poslinkius. Šiame straipsnyje yra pateiktas pavyzdys, kaip formos atminties lydinį panaudoti kaip šešiakojo žingsniuojančiojo roboto aktuatorių. Analizuojamas kojos mechanizmas, kuris šių aktuatorių sukuriamas mažas deformacijas gali keisti į nemažus poslinkius.

I. Doroftei, B. Stirbu

APPLICATION OF Ni-Ti SHAPE MEMORY ALLOY ACTUATORS IN A WALKING MICRO-ROBOT

S u m m a r y

As walking robots are requested to perform tasks in rough terrain, the development of actuators capable to flexibly adapt to the unstructured environment becomes more and more necessary. The conventional mechanisms with stiff joints make the robots more complex, heavy, large and expensive. Shape Memory Alloys are a category of artificial muscles which can be used as actuators for a walking robot. Even if they can exhibit large changes in shape when heated and cooled, only one part of their deformation can be used, if we want to maximize the actuator life. This is why smart mechanisms that can convert the small strain of the wire into large motion are necessary. In this paper, an example of using Shape Memory Alloys as actuators for a hexapod walking micro-robot is presented. A leg mechanism that can convert the small strain of these actuators in large motion is also discussed.

Keywords: flexible actuator, shape memory alloy, walking micro-robot, design**.**

Received February 20, 2013
Accepted January 21, 2014